



HAL
open science

Rational, Facile Synthesis and Characterization of the Neutral Mixed-Metal Organometallic Oxides

$\text{Cp}^*_2\text{MoxW}_{6-x}\text{O}_{17}$ ($\text{Cp}^* = \text{C}_5\text{Me}_5$, $x = 0, 2, 4, 6$)

Gülnur Taban-Çalışkan, Dominique Agustin, Funda Demirhan, Laure
Vendier, Rinaldo Poli

► To cite this version:

Gülnur Taban-Çalışkan, Dominique Agustin, Funda Demirhan, Laure Vendier, Rinaldo Poli. Rational, Facile Synthesis and Characterization of the Neutral Mixed-Metal Organometallic Oxides $\text{Cp}^*_2\text{MoxW}_{6-x}\text{O}_{17}$ ($\text{Cp}^* = \text{C}_5\text{Me}_5$, $x = 0, 2, 4, 6$). *European Journal of Inorganic Chemistry*, 2009, 2009 (34), pp.5219-5226. 10.1002/ejic.200900676 . hal-03184169

HAL Id: hal-03184169

<https://hal.science/hal-03184169>

Submitted on 29 Mar 2021

HAL is a multi-disciplinary open access archive for the deposit and dissemination of scientific research documents, whether they are published or not. The documents may come from teaching and research institutions in France or abroad, or from public or private research centers.

L'archive ouverte pluridisciplinaire **HAL**, est destinée au dépôt et à la diffusion de documents scientifiques de niveau recherche, publiés ou non, émanant des établissements d'enseignement et de recherche français ou étrangers, des laboratoires publics ou privés.

Rational, facile synthesis and characterization of the neutral mixed-metal organometallic oxides $\text{Cp}^*\text{M}_2\text{Mo}_x\text{W}_{6-x}\text{O}_{17}$ ($\text{Cp}^* = \text{C}_5\text{Me}_5$, $x = 0, 2, 4, 6$)

Gülnur Taban-Çalışkan,^[a,b,c] Dominique Agustin,^{*,[a,b]} Funda Demirhan,^{*,[c]} Laure Vendier,^[a] and Rinaldo Poli^{*,[a,d]}

Keywords: Organometallic oxides / tungsten / molybdenum / polyoxometallates / DFT calculation / X-ray powder analysis

The reaction of the bis(pentamethylcyclopentadienyl)pentaoxodimetal complexes $\text{Cp}^*\text{M}_2\text{O}_5$ with four equivalents of $\text{Na}_2\text{M}'\text{O}_4$ ($\text{M}, \text{M}' = \text{Mo}, \text{W}$) in acidic aqueous medium constitutes a soft and selective entry into neutral Lindqvist-type hexametallate organometallic mixed oxides $\text{Cp}^*\text{M}_2\text{Mo}_x\text{W}_{6-x}\text{O}_{17}$ ($x = 6$ (**1**), 4 (**2**), 2 (**3**), 0 (**4**)). The identity of the complexes is demonstrated by elemental analyses, thermogravimetric analyses and infrared spectroscopy. Thermal degradation of **1-4** up to $> 500^\circ\text{C}$ leads to $\text{Mo}_x\text{W}_{1-x}\text{O}_3$. The molecular identity and geometry of compound

2 is further confirmed by a fit of the powder X-ray diffraction pattern with a model obtained from previously reported single crystal X-ray structures of **1** and **4**, with which **2** is isomorphous. DFT calculations on models obtained by replacing Cp^* with Cp (**I-IV**) validate the structural assignments and assist in the assignment of the $\text{M}, \text{M}'\text{-O}$ vibrations.

- [a] CNRS; LCC (Laboratoire de Chimie de Coordination); Université de Toulouse; UPS, INPT; 205, route de Narbonne, F-31077 Toulouse, France
Fax: (+) 33-561553003
E-mail: rinaldo.poli@lcc-toulouse.fr
- [b] Université de Toulouse; Institut Universitaire de Technologie Paul Sabatier; Département de Chimie; Av. Georges Pompidou, BP 20258, F-81104 Castres Cedex, France
Fax: (+) 33-563356388
E-mail: dominique.agustin@iut-tlse3.fr
- [c] Celal Bayar University, Faculty of Sciences & Liberal Arts, Department of Chemistry, 45030 Muradiye-Manisa, Turkey
Fax: (+) 90-02362412158
E-mail: funda.demirhan@bayar.edu.tr
- [d] Institut Universitaire de France, 103, bd Saint-Michel, 75005 Paris, France.
-  Supporting information for this article is available on the WWW under <http://www.eurjic.org/> or from the author.

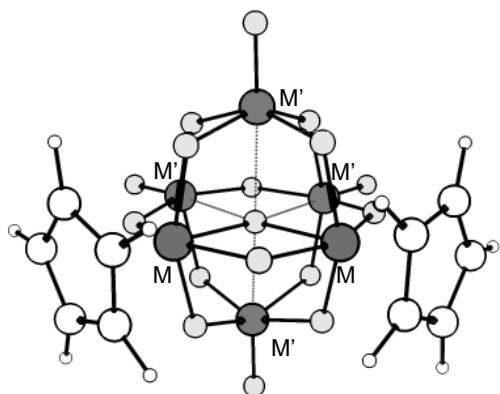
grafting of simple organic fragments on lacunary oxoclusters.^[14, 21-29] Hydrothermal synthesis from elementary bricks is also an alternative, though limited by serendipity.^[30, 31] Some of these syntheses lead to heterometallic species but need to be performed in specific environment, *i.e.* under argon, or under pressure, or using very sensitive species. Stability and/or compatibility with protic reagents and solvents are also useful for applications in “non-innocent” aqueous media. The introduction of organometallic moieties in a POM framework has attracted considerable attention,^[13, 32-38] because the organometallic fragment may impart new reactivity to the molecule relative to the all-inorganic equivalents. This strategy also allows the selective assembly of mixed-metal clusters under mild conditions, often using aqueous solvents. Specifically, the reaction of Na_2MO_4 ($\text{M} = \text{Mo}, \text{W}$) with $[\text{Cp}^*\text{RhCl}_2]_2$ or $[(\eta^6\text{-arene})\text{RuCl}_2]_2$ in water or acetonitrile yielded the octanuclear compounds $[(\text{LM})(\text{MoO})(\mu\text{-O})_3]_4$ [$\text{LM} = \text{Cp}^*\text{Rh}^{[32]}$ and $(p\text{-MeC}_4\text{H}_4\text{iPr})\text{Ru}^{[33]}$] and the tungsten analogues $[(\eta^6\text{-arene})\text{Ru}_4(\text{WO})_4(\mu\text{-O})_{12}]$ (arene = C_6Me_6 , $p\text{MeC}_6\text{H}_4\text{iPr}$).^[38]

Introduction

Mixed oxides containing two or more different metals attract interest because of a number of different applications in heterogeneous catalysis^[1-7] and in the elaboration of chromogenic materials,^[8] the advantage being the tunability of the desired property (reactivity, light absorption, ...) by modification of the nature and relative proportion of the different metals. A drawback is the difficulty to obtain materials with a homogeneous metal distribution at the atomic level by the currently applied techniques (sputtering, CVD).^[9] For catalytic applications, the use of polyoxometallates (POMs) can provide a “molecular scale” model for a better understanding of the interaction between the substrates and the oxide surface.^[10-12] For several decades, polyoxometallic species have attracted much interest because of their great versatility, with applications from biology to materials science and catalysis.^[13] Numerous research groups worldwide have specialized in the synthesis of these molecules with fine control of shape, size and elemental composition.^[13, 14] One synthetic strategy employs the assembly of predefined polyatomic fragments, often performed in organic solvents and with air- and water-sensitive organometallic precursors.^[13, 15-20] Another method uses the

We have worked extensively on the aqueous chemistry of the air-stable organometallic complexes $\text{Cp}^*\text{M}_2\text{O}_5$ ($\text{M} = \text{Mo}, \text{W}$)^[39-50] and have recently reported the synthesis and structure of $\text{Cp}^*\text{M}_2\text{Mo}_6\text{O}_{17}$, **1**.^[51] This is a hexanuclear organopolyoxometallic species with a Lindqvist-type octahedral arrangement of the six Mo atoms, as shown in Scheme 1. Each Mo atom bears a terminal Cp^* or oxo group, all edges of the octahedron are oxo-bridged, and there is an additional central ($\mu_6\text{-O}$) atom bonded to all Mo centers, thus the formula can be written as $[(\text{Cp}^*\text{M})_2(\text{MoO})_4(\mu_2\text{-O})_{12}(\mu_6\text{-O})]$. It is isoelectronic with the $[\text{Cp}^*\text{Mo}_6\text{O}_{18}]^-$ and $[\text{Mo}_6\text{O}_{19}]^{2-}$ ions.^[52-55] Small amounts of crystals suitable for a structural determination were obtained by a serendipitous slow decomposition of $\text{Cp}^*\text{M}_2\text{Mo}_2\text{O}_5$ under strong acidic conditions, but the selective and high yield synthesis was achieved by condensation of $\text{Cp}^*\text{M}_2\text{Mo}_2\text{O}_5$ with four equivalents of Na_2MoO_4 under acidic conditions. The identity and purity of the microcrystalline powder was confirmed by comparison of the X-ray powder diffraction spectrum with that simulated from the single crystal data. On the basis of this finding, we set out to extend this strategy to the full series of $[(\text{Cp}^*\text{M})_2(\text{M}'\text{O})_2(\mu_2\text{-O})_4(\mu_6\text{-O})]$

O)₁₂(μ₆-O)] complexes with M, M' = Mo, W, including the previously unknown mixed-metal species. The M = M' = W compound, Cp*₂W₆O₁₇, has previously been described but was only obtained as “major oxidation product” from a sealed-tube reaction between [Cp*W(CO)₂]₂ and the arsaoxane impurity in the cyclic polysilane *c*-(AsCH₃)₅ as oxygen transfer agent.^[56] As described herein, the same synthetic protocol leads to the full series of Cp*₂M₂M'₄O₁₇ compounds.

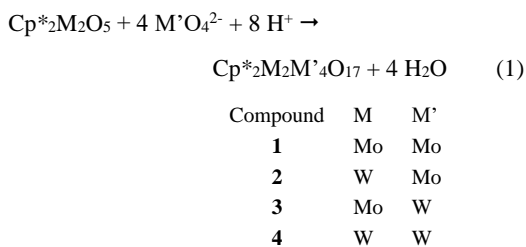


Scheme 1. Structure of the [(Cp*M)₂(M'O)₄(μ₂-O)₁₂(μ₆-O)] compounds (M, M' = Mo, W).

Results and Discussion

(a) Synthesis

The reaction between Cp*₂M₂O₅ and M'O₄²⁻ (M, M' = Mo, W), under the conditions previously described for the synthesis of the Mo₆ derivative **1**,^[51] yield all other three complexes in excellent yields and purity, see equation 1.



Mixing a methanolic solution of Cp*₂M₂O₅ (this compound is insoluble in pure water but soluble in aqueous methanol solutions) and an aqueous solution of Na₂M'O₄ (4 equiv) yields the products as fine precipitates immediately after acidification. The compound colour varies from orange-brown to yellow-green, depending on the Mo/W ratio. Direct contact with metallic materials (i.e. syringe needles or spatulas) causes reduction with strong darkening of the compounds colour towards green and should therefore be avoided.

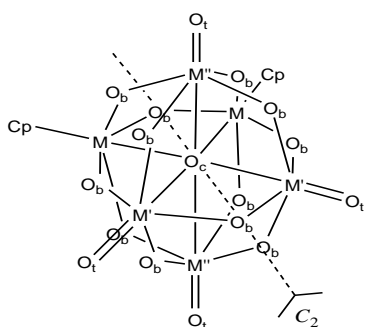
Previous work in our group has shown that the Cp*-Mo bond in Cp*₂Mo₂O₅ is quite robust and withstands exposure to aqueous media in the entire pH range, at least for reasonably long periods of time.^[39] Analogous studies for the W analogue have not been carried out, but W-ligand bonds are usually stronger than the Mo congeners. Thus, it is not surprising that the Cp*M moieties are transferred intact from the Cp*₂M₂O₅ starting materials to the products. Our previous studies have also shown that Cp*₂Mo₂O₅ ionizes in water and yields the species Cp*MoO₂⁺ and Cp*MoO₂(H₂O)⁺ at low pH.^[39, 57] Once again, the behaviour under

the same conditions of the W analogue has not been investigated but can be assumed to parallel that of Mo. Thus, the synthesis can be seen as the assembly of individual organometallic Cp*MoO₂⁺ and inorganic M'O₄²⁻ species, regulated by stoichiometry and pH. The products are stable in water at low pH. Upon raising the pH, however, the solid redissolves in the medium, slowly at pH 6, faster at higher pH, possibly regenerating a mixture of the starting materials (the formation of Cp*₂Mo₂O₅ was confirmed by IR on the isolated residue). Unfortunately, the compounds are too little soluble in common solvents for characterization by techniques such as NMR or electrochemistry, but they could be characterized by solid state analytical methods (IR, TGA and powder X-ray diffraction, *vide infra*)

(b) DFT calculations

DFT geometry optimizations were carried out for the purpose of assigning the IR absorption bands and interpreting the effect on them of the metal nature. To save computational time, the calculations were run on simplified models (indicated by roman numerals corresponding to the compounds numbering scheme) where the Cp* ligands were replaced by Cp rings. Before examining these results, we present a brief description of the optimized geometries. The results are collected in **Table 1**. Since the four M' atoms occupy structurally distinct positions, we shall distinguish them by introducing the M'₂M''₂ notation, limited to the structural description. The agreement between experimental and calculated geometries for the M₂M'₂M''₂O₁₇ core is generally very good, including the asymmetry of the M-O_b, M'-O_b and M''-O_b distances, which is more pronounced for the Mo₆ structure but experimentally visible also in some of the W₆ structural parameters. The reason for this distortion is not clear, but the computational method seems to confirm that the distortion is a molecular phenomenon, not related to crystal packing. The molecules are located on a crystallographic twofold axis, as shown in **Scheme 2**, thus each pair of M'=O_t, M''=O_t, M-O_c, M'-O_c and M''-O_c bonds are equivalent by symmetry. Although the geometry optimizations were carried out without any symmetry constraints, this twofold symmetry was essentially maintained in the optimized geometries. The calculated distances to the terminal and bridging ligands are generally only slightly longer than those experimentally observed (maximum deviation 0.04 Å for M-O_{M'} in **I**), whereas the distances to the central O atom are underestimated for M-O_c (by 0.01 Å in **I** and by 0.06 Å in **IV**) and overestimated for M'-O_c and M''-O_c (by up to 0.11 Å in **IV**). Note that O_c is much closer to M than to M' and M'' and that the calculations tend to place O_c even closer to M relative to the experimental structure, which could be related to the use of the simplified model.

After establishing the suitability of this level of theory to reproduce the structural features, it is now interesting to examine some specific trends along the series of the optimized structures. The M'=O_t and M''=O_t distances slightly lengthen on going from Mo to W. All distances to O_c, on the other hand, shorten on going from Mo to W. No clear trends can be established for the distances to the O_b atoms because of the asymmetry caused by the distortion from C_{2v} symmetry. It is also difficult to establish whether there are secondary effects, for instance of the nature of M' and M'' on the M-O_b distances. Going from Mo to W for M' and M'' seems to lead to M-O_c shortening, whereas no significant change is visible on the M'=O_t and M''=O_t distances by the nature of M. Given the sensitivity of the DFT optimization procedure, we do not consider differences at the level of the third significant digit as reliable. Secondary effects will be more clearly revealed by the IR study.



Scheme 2. Atom labelling scheme used in Table 1.

Table 1. Selected bonding distances for the geometry optimized models **I-IV** and comparison with the experimental structures of **1** and **4**.^[a]

System	1 ^[b]	I	II	III	IV	4 ^[c]
(M, M'=M'')	(Mo,Mo)	(Mo,Mo)	(W,Mo)	(Mo,W)	(W,W)	(W,W)
Cp-M	2.109(5)	2.13	2.14	2.12	2.13	2.11(4)
M ^z -O _t	1.687(3)	1.68	1.68	1.69	1.69	1.69(2)
M ^{z'} -O _t	1.683(3)	1.68	1.68	1.70	1.70	1.69(2)
M-O _c	2.145(2)	2.13	2.12	2.15	2.14	2.20(1)
M ^z -O _c	2.542(3)	2.62	2.62	2.60	2.61	2.50(2)
M ^{z'} -O _c	2.3674(5)	2.41	2.41	2.39	2.39	2.36(2)
M-O _{b(M)}	1.943(2)	1.95	1.95	1.95	1.94	1.93(1)
M-O _{b(M')}	1.955(3)	1.92	1.92	1.93	1.92	1.94(2)
M-O _{b(M'')}	2.029(3)	2.04	1.99	1.95	1.94	1.97(2)
M ^z -O _{b(M)}	1.890(3)	1.86	1.88	1.93	1.93	1.92(2)
M ^z -O _{b(M')}	1.883(3)	1.93	1.93	1.92	1.92	1.89(2)
M ^z -O _{b(M'')}	1.916(2)	1.91	1.91	1.92	1.91	1.92(1)
M ^{z'} -O _{b(M)}	1.977(3)	2.00	1.99	1.93	1.92	1.93(2)
M ^{z'} -O _{b(M')}	1.861(3)	1.86	1.86	1.92	1.92	1.92(2)
M ^{z'} -O _{b(M'')}	1.980(3)	2.02	1.89	1.93	1.94	1.93(2)
M ^{z''} -O _{b(M)}	1.855(3)	1.86	2.00	1.94	1.94	1.92(2)
M ^{z''} -O _{b(M')}	2.006(3)	2.01	1.99	1.93	1.92	1.94(2)
M ^{z''} -O _{b(M'')}	1.871(3)	1.86	1.87	1.92	1.92	1.94(2)

[a] For the definition of the symbols used, see Scheme 2. [b] From the X-ray structure published in ref. ^[51]. [c] From the X-ray structure published in ref. ^[56].

(c) IR characterization

Infrared spectroscopy is a good characterization tool for polyanions, especially when they possess high symmetry such as the M₆O₁₉²⁻ Lindqvist anions (M= Mo, W).^[58, 59] The number of vibrations observed for salts of these anions agree with the *O_h* space group and a correlation between experimental and calculated spectrum could be established.^[60] As already discussed above, the symmetry of systems **1-4** is reduced to *C₂* (considering Cp* as a rapidly rotating ligand), with an ideal *C_{2v}* symmetry if the M-O_b, M^z-O_b and M^{z'}-O_b asymmetry is averaged.

The observed (for **1-4**) and calculated (for **I-IV**) IR spectra in the metal-oxygen stretching region are shown in **Figure 1** and the most prominent absorptions are listed in **Table 2** (calculated) and (experimental). Views of the normal modes of vibrations corresponding to these calculated bands are available in the Supporting Information. The terminal M^z-O_t and M^{z'}-O_t vibrations are in the higher frequency part of the spectrum (observed, 950-1000 cm⁻¹; calculated, 1020-1050 cm⁻¹), whereas the vibrations involving the O_b atoms are in the 750-850 cm⁻¹ range. A few Cp C-C in-plane and C-H out-of-plane bending motions are

also present in this region (840-960 cm⁻¹) but have low intensity and do not significantly contribute to the calculated spectrum. The match between calculated and observed spectra is satisfactory, the frequency difference being related to either the computational method or to the model (Cp vs. Cp*) or to a combination of both. The observed and calculated relative intensities, on the other hand, match rather well, giving us confidence in the assignment of the observed bands.

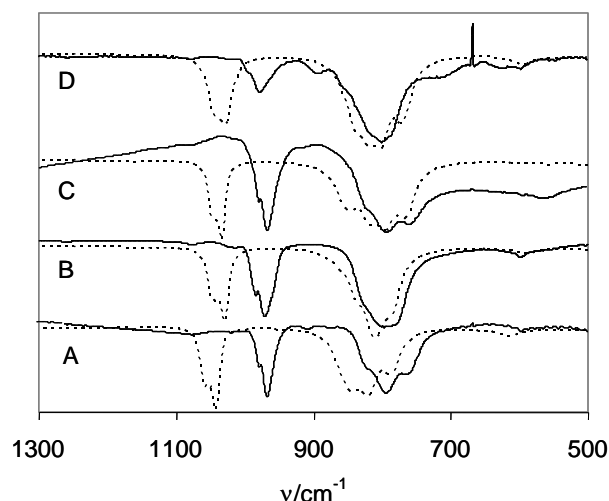


Figure 1. Experimental (plain lines) and DFT calculated (unscaled, dotted lines) IR spectra in the Mo-O stretching region for compounds **1/I** (A), **2/II** (B), **3/III** (C), **4/IV** (D).

Table 2. Calculated metal-O vibrations (cm⁻¹) in the 700-1100 cm⁻¹ region with relative intensities (KM/Mole) in parentheses.

Type ^[a]	I	II	III	IV	Assignment
<i>b</i> ₁	770 (723)	786 (879)	766 (803)	785 (927)	<i>v</i> _{as} [M-O-Mt] ^[b]
	801 (853)	807 (820)	795 (859)	809 (927)	<i>v</i> _{as} [M-O-M'+M-O-M'']
<i>b</i> ₂	820 (661)	815 (688)	818 (734)	821 (765)	<i>v</i> [Mt-O-Mt] ^[b]
	838 (283)	836 (350)	845 (268)	848 (273)	<i>v</i> [Mt-O-Mt] ^[b]
<i>a</i> ₁	839 (291)	838 (218)	854 (399)	856 (159)	<i>v</i> [Mt-O-Mt] ^[b]
	1027 (484)	1029 (497)	1033 (389)	1036 (389)	<i>v</i> _{as} (M''=O)
<i>a</i> ₁	1030 (15)	1032 (19)	1036 (13)	1038 (15)	<i>v</i> _s (M'=O) [- <i>v</i> _s (M'=O)]
	1038 (212)	1040 (213)	1042 (163)	1044 (163)	<i>v</i> _{as} (M'=O)
<i>b</i> ₂	1046 (280)	1048 (274)	1048 (215)	1050 (201)	<i>v</i> _s (M'=O) [+ <i>v</i> _s (M''=O)]

[a] Under idealized *C_{2v}* symmetry. [b] Mt = M, M' and M''.

Table 3. Observed metal-O vibrations (cm⁻¹) in the 700-1100 cm⁻¹ region.

1	2	3	4	Assignment
764m	780s	760s	789sh	<i>v</i> [Mt-O-Mt]
794s	797s	793s	799s	<i>v</i> [Mt-O-Mt]
820m	825sh	820sh	820sh	<i>v</i> [Mt-O-Mt]
968s	971s	967s	977s	<i>v</i> _{as} (M''=O)
980m	984m	979m	994m	<i>v</i> (M'=O)

We can now discuss with confidence the frequency trends related to the metal changes. First of all, the nature of the normal modes for the bands associated to the O_b atoms does not allow a

fine analysis of the distortion from the ideal C_{2v} to the observed C_2 symmetry, thus the higher symmetry point group labels are used in **Table 2** and in the discussion. Four terminal metal-oxido ($M'=O_t$ and $M''=O_t$) vibrations are expected and indeed calculated. One of them, $\nu_s(M'=O)$, is very weak because the two bonds are essentially co-linear and the overall dipole moment change is small. The small intensity is due to the deviation from co-linearity and to a small vibrational coupling with the $\nu_s(M'=O)$ vibration, also of a_1 type (see Figure in the Supporting Information). Thus, only three major bands are essentially observed in this region. The calculated frequencies show both a primary and a secondary effect. As M' and M'' go from Mo (**I/II**) to W (**III/IV**), all four frequencies experience a blue-shift. However, a blue shift is also caused by the secondary effect of changing M from Mo (**I/III**) to W (**II/IV**). From the experimental spectra only two $\nu(M=O)$ bands can be unambiguously determined. Comparison with the calculated spectra suggest that the strongest one is $\nu_{as}(M''=O)$, whereas the second smaller band is most probably the highest frequency a_1 band. The determination of the band positions is less accurate because of the broadening and resolution, but the same trends observed for the calculated bands appears to be observed, the primary effect being most evident in the **2/4** comparison, while the secondary effect is clearly evident in both **1/2** and **3/4** comparisons. The 12 metal-(bridging O atom) bonds yield in principle 12 normal modes, but only 5 of the 6 asymmetric motions can be clearly identified for the calculated spectrum (and 3 in the observed spectrum) in the typical “fingerprint region”, while the symmetric motions are located at lower frequency and combined with other types of vibrations. These bands also shift to higher frequency when one or both metals directly implicated in the bond(s) is(are) changed from Mo to W. Experimentally, the most significant change in this region is seen for a change of the inorganic metal, whereas a change of the organometallic one produces hardly any change. For the $a_1 \nu[Mt-O-Mt]$ band, which has the main contribution from M' and M'' , the secondary effect of changing M is small. All other observed bands involve a combination of $M-O_b$ on one side and $M'-O_b$ or $M''-O_b$ on the other side, thus a distinction of primary and secondary effects is not possible.

(d) TGA measurements

All compounds lead to complete loss of the organic part, with a good match between experimentally observed and theoretical mass losses on the basis of equation 2, upon warming up to 600°C in thermogravimetric experiments conducted in air. The spectrograms for the TGA of compounds **1** and **3** are shown in Figure 2, while those of **2** and **4** are given in the Supporting Information. The onset of Cp* ligands loss occurs at lower temperatures for **1** (190°C) and **3** (230°C) where these ligands are bonded to Mo, whereas higher temperatures are necessary to induce loss of the Cp* bonded to W (270°C for **2**, 310°C for **4**). A secondary effect of the inorganic metal, however, is notable by comparing these temperatures for the **1/2** and **3/4** couples. Interestingly, the two Cp* rings are lost in two quite distinct and sharp steps for compound **1**, whereas a more gradual loss within a broader temperature range is observed for the other three compounds. The resulting residues from **1** and **4** had the expected colour (white for MoO_3 , yellow for WO_3). The final product of the thermal decomposition from **2** and **3** is thus a mixed-metal oxide material with controlled metal composition, $Mo_{2/3}W_{1/3}O_3$ and $Mo_{1/3}W_{2/3}O_3$, respectively.

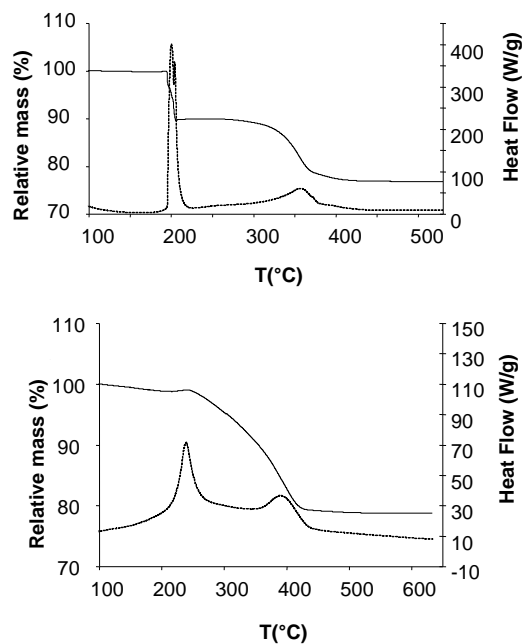
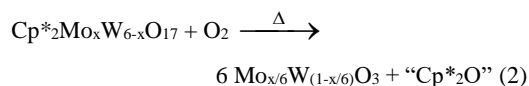


Figure 2. Spectrogram for the TGA of compounds **1** (above) and **3** (below). The solid curves correspond to the percent weight loss (left y axes) and the dashed curves to the heat flow (right y axes).

(e) X-ray powder diffraction

As mentioned in the introduction, single crystal X-ray structures have already been determined for compounds **1** and **4**^[51, 56] and shown to be isomorphous (monoclinic $C_{2/c}$) with very similar unit cell parameters. We therefore considered that the same crystal system may also be adopted by the mixed-metal compounds **2** and **3**. Furthermore, a powder diffraction study was also reported for compound **1**, as obtained in microcrystalline form by the same condensation process of equation 1 in aqueous solution, and shown to match with the pattern calculated from the single crystal data.^[51] Thus, we have proceeded to measure powder X-ray diffraction patterns for compounds **2** and **3**. Compound **2** was obtained in sufficient microcrystalline quality to give a well resolved powder spectrum, which is shown in **Figure 3**. This pattern was compared with that calculated from the model obtained by changing the M atoms from Mo to W in the known X-ray structure of compound **1**. All measured peaks are accounted for by the model, showing that the sample does not contain any other diffracting phases. All subsequent attempts to refine the atom positions, even when restricted only to the metal atoms, did not lead to convergence. This is probably due to the transmission geometry used for recording the diffracted intensities. Indeed, since it was difficult to synthesise high quantity of powder (necessary for working in reflection mode), we used the transmission mode on capillary sample and the high absorption prevented a good simulation of the diffracted intensities. The diffraction geometry also resulted in high peak asymmetry, as most clearly visible for the most intense peaks at low angles. However, free refinement of the metal atoms thermal parameters and of a common thermal parameter for the C and O atoms gave very reasonable values, with $R = 5.14$, $R_p = 17.8$, $R_{wp} = 17.8$, and a Bragg R factor of 13.82. It is notable that refinement of all other possible models corresponding to the metal placement as expected for **1**, **3** and **4** gave unreasonably small (when the W position was modelled by Mo) or high (when the Mo position was modelled by W) thermal parameters. Figures of these refined structures are shown in the SI. The R factors for the three wrong models were slightly greater (**1**: 6.28 %; **3**: 9.04 %; **4**: 6.51 %) than

for the correct model. Thus, the powder X-ray diffraction experiment provides strong evidence that compound **2** has the same structure previously determined for **1** and **4**, with Mo occupying solely the inorganic sites and W occupying solely the organometallic sites. The same conclusions concerning the structure and the site selectivity can reasonably be assumed for compound **3**.

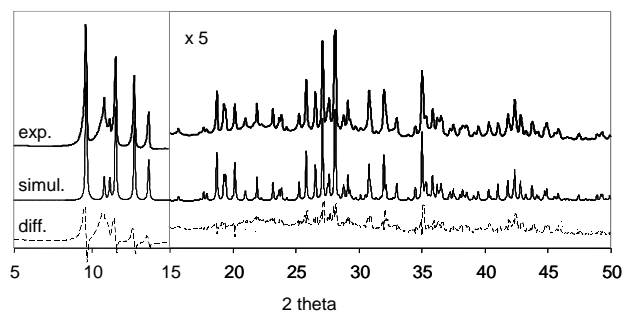


Figure 3. Powder X-ray diffraction patterns for compound **2**. Bold plain line (above): experimental spectrum; plain line (middle): simulated spectrum; dashed line (below): difference.

Conclusions

We have presented here a rational and facile synthesis of organometallic Lindqvist-type polyoxo(Group 6 metal) compounds of type $\text{Cp}^*_2\text{M}_2\text{M}'_4\text{O}_{17}$ ($\text{M} = \text{Mo}, \text{W}$). This route, already known for the $\text{M} = \text{M}' = \text{Mo}$ member (compound **1**), has now been extended to afford a high-yield selective synthesis of the already known $\text{M} = \text{M}' = \text{W}$ member (compound **4**) and also to prepare the previously unknown mixed metal systems. Thermal decomposition of these compounds has been shown to yield mixed-metal oxides $\text{Mo}_{2/3}\text{W}_{1/3}\text{O}_3$ and $\text{Mo}_{1/3}\text{W}_{2/3}\text{O}_3$ with an expected homogeneous distribution of the two metals, which may be of interest for the study of the metal influence in heterogeneous catalytic as well as in chromogenic applications.

Experimental Section

All experiments were performed in air. Compounds $\text{Cp}^*_2\text{Mo}_2\text{O}_5$ and $\text{Cp}^*_2\text{W}_2\text{O}_5$ were synthesized according to the literature.^[48] Water was deionized and methanol (Carlo Erba, analytical grade) was used as received. Sodium tungstate dihydrate ($\text{Na}_2\text{WO}_4 \cdot 2\text{H}_2\text{O}$) and sodium molybdate dihydrate ($\text{Na}_2\text{MoO}_4 \cdot 2\text{H}_2\text{O}$) were purchased from Aldrich and used as received. Elemental analyses (C, H and O) were performed by the LCC Analytical Service Laboratory. The IR spectra were recorded on KBr pellets at room temperature with a Mattson Genesis II FTIR spectrometer and the data were processed with WinFirst software. The TGA measurements were carried out on a SDT Q600 V20.9 thermal analyzer. A quantity of each sample was placed into a nickel/platinum alloy crucible and heated at $0.83 \text{ K}\cdot\text{s}^{-1}$ under reconstituted air flow up to 600 K. An empty crucible was used as a reference.

Synthesis of $\text{Cp}^*_2\text{Mo}_6\text{O}_{17}$, **1.** This procedure follows that reported previously, except that the latter contains a typographical error in the amount of acid used.^[51] Thus, using $\text{Cp}^*_2\text{Mo}_2\text{O}_5$ (27 mg, $5.0 \cdot 10^{-2}$ mmol) in 1.25 mL of MeOH, $\text{Na}_2\text{MoO}_4 \cdot 2\text{H}_2\text{O}$ (48.4 mg, 0.20 mmol) in 1.25 mL of water, and a 1 M HNO_3 solution (0.4 mL, 0.4 mmol), led to 23.5 mg of product (62% yield). The IR spectrum matched that previously reported. Anal. for $\text{C}_{20}\text{H}_{30}\text{Mo}_6\text{O}_{17}$ (1118.08): C, 21.44 (21.48); H, 2.60 (2.70). calcd C 21.48, H 2.70; found C 21.44, H 2.60. TGA, loss of Cp^* and uptake of O, % exp. (calcd): 23.1 (22.7).

Synthesis of $\text{Cp}^*_2\text{W}_2\text{Mo}_4\text{O}_{17}$, **2.** $\text{Cp}^*_2\text{W}_2\text{O}_5$ (30 mg, $4.18 \cdot 10^{-2}$ mmol) was dissolved in 2 mL of MeOH. Separately, $\text{Na}_2\text{MoO}_4 \cdot 2\text{H}_2\text{O}$ (40 mg, 0.167 mmol) was dissolved in 2 mL of water. The two solutions were mixed without apparent change. A 1 M HNO_3 solution (0.75 mL, 0.75 mmol) was then slowly added, forcing the immediate formation of a dark yellow precipitate, which became paler yellow after ca. 1 h. After stirring overnight at room temperature, the solid was filtered, washed H_2O , then with MeOH (where it is sparingly soluble), and finally dried at 70°C (38.5 mg, 71.3% yield). IR (KBr pellets, cm^{-1}): 1496s, 1442s, 1377s, 1081s, 1024sh, 984sh, 972s, 828sh, 801s, 785sh, 600s. Anal for $\text{C}_{20}\text{H}_{30}\text{W}_2\text{Mo}_4\text{O}_{17}$ (1293.88): calcd C 18.56; H 2.34; found C, 18.47, H 1.73. TGA loss of Cp^* and uptake of O, % exp. (calcd): 19.3 (19.6).

Synthesis of $\text{Cp}^*_2\text{Mo}_2\text{W}_4\text{O}_{17}$, **3.** $\text{Cp}^*_2\text{Mo}_2\text{O}_5$ (54.2 mg, 0.1 mmol) was dissolved in 2.5 mL of MeOH. Separately, $\text{Na}_2\text{WO}_4 \cdot 2\text{H}_2\text{O}$ (131.9 mg, 0.4 mmol) was dissolved in 2.5 mL of water. The two solutions were mixed with no apparent change. A 1 M HNO_3 solution (1.8 mL, 1.8 mmol) was slowly added, forcing the immediate formation of a bright orange precipitate that darkens with time until green. The mixture was stirred overnight. The solid was filtered, and finally dried at 70°C under vacuum. The powder has been then washed with diethylether to remove unreacted $\text{Cp}^*_2\text{Mo}_2\text{O}_5$. (yield: 86.5 mg, 15%). IR (KBr pellets, cm^{-1}): 1491s, 1444s, 1376s, 1265w, 1173w, 1093w, 972s, 920sh, 890sh, 851sh, 809s, 767sh, 706s, 610s, 546s. Anal for $\text{C}_{20}\text{H}_{30}\text{Mo}_2\text{W}_4\text{O}_{17}$ (1469.68): calcd C 16.34, H 2.06; found C 16.68, H 1.70. TGA loss of Cp^* and uptake of O, % exp. (calcd): 19.7 (17.3).

Synthesis of $\text{Cp}^*_2\text{W}_6\text{O}_{17}$, **4.** $\text{Cp}^*_2\text{W}_2\text{O}_5$ (30 mg, $4.2 \cdot 10^{-2}$ mmol) was dissolved in 2 mL of MeOH. Separately, $\text{Na}_2\text{WO}_4 \cdot 2\text{H}_2\text{O}$ (55 mg, 0.17 mmol) was dissolved in 1.5 mL of water. The two solutions were mixed with no apparent change. A 1 M HNO_3 solution (0.33 mL, 330 μmol) was slowly added, forcing the immediate precipitation of a yellow-white powder. The mixture was stirred for one day, and then the yellow solid was filtrated, washed with H_2O , then with MeOH, and finally dried at 70°C under vacuum (46.4 mg, 67.5% yield). IR (KBr pellets, cm^{-1}): 1498s, 1442s, 1376s, 996sh, 980s, 896sh, 806s, 741w, 600sh. Anal. for $\text{C}_{20}\text{H}_{30}\text{W}_6\text{O}_{17}$ (1645.48): calcd C 14.59, H, 1.83; found C 15.14, H 1.33. TGA loss of Cp^* and uptake of O, % exp. (calcd): 16.3 (15.4).

X-ray powder analyses. The XRD data was collected at room temperature using a theta/theta Panalytical MPdPro powder diffractometer, using Cu K_α radiation ($\lambda = 0.15406 \text{ nm}$), in transmission mode on a capillary sample. The XRD pattern was recorded with a step width of 0.016 and a counting time of 1000 s step^{-1} . The sample was measured over a 2θ range from $5^\circ \leq 2\theta \leq 70^\circ$. The indexation of the pattern, the fullprofile matching and the Rietveld refinement were performed using the Winplotr interface.^[61]

Computational Details. The guess geometries for **I** and **IV** were based on the crystallographically determined structures of **1** and **4**,^[51, 56] replacing all CH_3 groups by H atoms in the Cp^* ligands. From the resulting optimized geometries, starting geometries for **II** and **III** were generated by changing the metal. All optimizations were carried out on the gas phase isolated molecules using the Gaussian 03 suite of programs^[62] with the B3LYP functional, which includes the three-parameter gradient-corrected exchange functional of Becke^[63] and the correlation functional of Lee, Yang, and Parr.^[64, 65] The standard 6-31G** basis set was used for the C, H and O atoms, while the CEP-31G* basis set^[66] was adopted for Mo and W. We found that the commonly used LANL2DZ basis set on the metal atom, tested for system **I**, resulted in longer bond lengths than the CEP-31G* basis, with a greater difference relative to the experimental values, most likely because polarization functions were not added to the metal atom basis set. Analytical frequency calculations were also run on the optimized geometries, yielding positive frequencies for all normal modes. The calculated IR spectra shown in **Figure 1** were generated from the DFT-generated frequencies and intensities by applying Lorentzian functions and adjusting the linewidth to best fit the experimental spectra.

Supporting Information (see footnote on the first page of this article): Figures of normal vibrational modes, structural models for the X-ray diffraction of compound **2**, and TGA spectra of compounds **1**, **3** and **4** (4 pages).

Acknowledgments

We are grateful to the Centre National de la Recherche Scientifique and to a binational (France-Turkey) Bosphore programme for funding this research. We also thank the French Embassy in Ankara for financial support of the Ph.D. thesis of G.T.C.

- [1] G. Schimanke, M. Martin, J. Kunert and H. Vogel, *Z. Anorg. Allg. Chem.* **2005**, *631*, 1289-1296.
- [2] M. V. Landau, L. Vradman, A. Wolfson, P. M. Rao and M. Herskowitz, *C. R. Chimie* **2005**, *8*, 679-691.
- [3] G. Mestl, *Topics Cat.* **2006**, *38*, 69-82.
- [4] P. Kampe, L. Giebeler, D. Samuelis, J. Kunert, A. Drochner, F. Haass, A. H. Adams, J. Ott, S. Endres, G. Schimanke, T. Buhrmester, M. Martin, H. Fuess and H. Vogel, *Physical Chemistry Chemical Physics* **2007**, *9*, 3577-3589.
- [5] S. Endres, P. Kampe, J. Kunert, A. Drochner and H. Vogel, *Appl. Catal. A* **2007**, *325*, 237-243.
- [6] W. A. Goddard, K. Chenoweth, S. Pudar, A. C. T. Van Duin and M. J. Cheng, *Topics Cat.* **2008**, *50*, 2-18.
- [7] N. R. Shiju and V. V. Gulians, *Appl. Catal. A* **2009**, *356*, 1-17.
- [8] S. H. Baeck, T. F. Jaramillo, D. H. Jeong and E. W. McFarland, *Chem. Commun.* **2004**, 390-391.
- [9] J. Kunert, A. Drochner, J. Ott, H. Vogel and H. Fuess, *Appl. Catal. A* **2004**, *269*, 53-61.
- [10] D. Masure, P. Chaquin, C. Louis, M. Che and M. Fournier, *J. Catal.* **1989**, *119*, 415-425.
- [11] N. Mizuno, *Trends Phys. Chem.* **1994**, *4*, 349-362.
- [12] T. Kim, A. Burrows, C. J. Kiely and I. E. Wachs, *J. Catal.* **2007**, *246*, 370-381.
- [13] P. Gouzerh and A. Proust, *Chem. Rev.* **1998**, *98*, 77-111.
- [14] A. Proust, R. Thouvenot and P. Gouzerh, *Chem. Commun.* **2008**, 1837-1852.
- [15] R. K. C. Ho and W. G. Klemperer, *J. Am. Chem. Soc.* **1978**, *100*, 6772-6774.
- [16] W. G. Klemperer and W. Shum, *J.C.S. Chem. Commun.* **1979**, 60-61.
- [17] R. G. Finke, B. Rapko and P. J. Domaille, *Organometallics* **1986**, *5*, 175-178.
- [18] P. Gouzerh, Y. Jeannin, A. Proust and F. Robert, *Angew. Chem., Int. Ed. Engl.* **1989**, *28*, 1363-1364.
- [19] A. Proust, P. Gouzerh and F. Robert, *Inorg. Chem.* **1993**, *32*, 5291-5298.
- [20] T. Nagata, M. Pohl, H. Weiner and R. G. Finke, *Inorg. Chem.* **1997**, *36*, 1366-1377.
- [21] F. Zonnevijlle and M. T. Pope, *J. Am. Chem. Soc.* **1979**, *101*, 2731-2732.
- [22] W. H. Knoth, *J. Am. Chem. Soc.* **1979**, *101*, 759-760.
- [23] W. H. Knoth, *J. Am. Chem. Soc.* **1979**, *101*, 2211-2213.
- [24] P. Judeinstein, C. Deprun and L. Nadjó, *J. Chem. Soc., Dalton Trans.* **1991**, 1991-1997.
- [25] N. Ammari, G. Herve and R. Thouvenot, *New J. Chem.* **1991**, *15*, 607-608.
- [26] A. Mazeaud, N. Ammari, F. Robert and R. Thouvenot, *Angew. Chem., Int. Ed. Engl.* **1996**, *35*, 1961-1964.
- [27] D. Agustin, C. Coelho, A. Mazeaud, P. Herson, A. Proust and R. Thouvenot, *Z. Anorg. Allg. Chem.* **2004**, *630*, 2049-2053.
- [28] D. Agustin, J. Dallery, C. Coelho, A. Proust and R. Thouvenot, *J. Organomet. Chem.* **2007**, *692*, 746-754.
- [29] J. Li, I. Huth, L. M. Chamoreau, B. Hasenknopf, E. Lacote, S. Thorimbert and M. Malacria, *Angew. Chem., Int. Ed. Engl.* **2009**, *48*, 2035-2038.
- [30] K. Oshihara, Y. Nakamura, M. Sakuma and W. Ueda, *Catal. Today* **2001**, *71*, 153-159.
- [31] A. Dolbecq and F. Secheresse, *Advances in Inorganic Chemistry, Vol 53* **2002**, *53*, 1-40.
- [32] Y. Hayashi, K. Toriumi and K. Isobe, *J. Am. Chem. Soc.* **1988**, *110*, 3666-3668.
- [33] G. Suss-Fink, L. Plasseraud, V. Ferrand and H. Stoeckli-Evans, *Chem. Commun.* **1997**, 1657-1658.
- [34] P. Blenkinsop, A. J. Carty, S. M. Peng, G. H. Lee, C. J. Su, C. W. Shiu and Y. Chi, *Organometallics* **1997**, *16*, 519-521.
- [35] C. W. Shiu, Y. Chi, A. J. Carty, S. M. Peng and G. H. Lee, *Organometallics* **1997**, *16*, 5368-5371.
- [36] A. Proust, R. Thouvenot and P. Herson, *J. Chem. Soc., Dalton Trans.* **1999**, 51-55.
- [37] G. Suss-Fink, L. Plasseraud, V. Ferrand, S. Stanislas, A. Neels, H. Stoeckli-Evans, M. Henry, G. Laurenczy and R. Roulet, *Polyhedron* **1998**, *17*, 2817-2827.
- [38] V. Artero, A. Proust, P. Herson and P. Gouzerh, *Chem. Eur. J.* **2001**, *7*, 3901-3910.
- [39] E. Collange, J. Garcia and R. Poli, *New J. Chem.* **2002**, *26*, 1249-1256.
- [40] F. Demirhan, J. Gun, O. Lev, A. Modestov, R. Poli and P. Richard, *J. Chem. Soc., Dalton Trans.* **2002**, 2109-2111.
- [41] D. Saurenz, F. Demirhan, P. Richard, R. Poli and H. Sitzmann, *Eur. J. Inorg. Chem.* **2002**, 1415-1424.
- [42] E. Collange, F. Demirhan, J. Gun, O. Lev, A. Modestov, R. Poli, P. Richard and D. Saurenz in *Perspectives in Organometallic Chemistry, Vol. 287* (Ed.: C. G. Screttas), Royal Society of Chemistry, **2003**, pp. 167-182.
- [43] F. Demirhan, P. Richard and R. Poli, *Inorg. Chim. Acta* **2003**, *347*, 61-66.
- [44] R. Poli, *Chem. Eur. J.* **2004**, *10*, 332-341.
- [45] F. Demirhan, G. Taban, M. Baya, C. Dinoi, J.-C. Daran and R. Poli, *J. Organometal. Chem.* **2006**, *691*, 648-654.
- [46] F. Demirhan, B. Çağatay, D. Demir, M. Baya, J.-C. Daran and R. Poli, *Eur. J. Inorg. Chem.* **2006**, 757-764.
- [47] C. Dinoi, P. Prikhodchenko, F. Demirhan, J. Gun, O. Lev, J.-C. Daran and R. Poli, *J. Organomet. Chem.* **2007**, *692*, 2599-2605.
- [48] C. Dinoi, G. Taban, P. Sözen, F. Demirhan, J.-C. Daran and R. Poli, *J. Organomet. Chem.* **2007**, *692*, 3743-3749.
- [49] C. Dinoi, P. Sözen, G. Taban, D. Demir, F. Demirhan, P. Prikhodchenko, J. Gun, O. Lev, J.-C. Daran and R. Poli, *Eur. J. Inorg. Chem.* **2007**, 4306-4316.
- [50] R. Poli, *Coord. Chem. Rev.* **2008**, *252*, 1592-1612.
- [51] E. Collange, L. Metteau, P. Richard and R. Poli, *Polyhedron* **2004**, *23*, 2605-2610.
- [52] H. Allcock, E. Bissell and E. Shawl, *Inorg. Chem.* **1973**, *12*, 2963-2968.
- [53] C. Garner, N. Howlader, A. Mcphail, R. Miller, K. Onan and F. Mabbs, *J. Chem. Soc., Dalton Trans.* **1978**, 1582-1589.
- [54] J. Fuchs and K. F. Jahr, *Z. Naturforsch., Sect. B* **1968**, *23*, 1380.
- [55] F. Bottomley and J. Chen, *Organometallics* **1992**, *11*, 3404-3411.
- [56] J. R. Harper and A. L. Rheingold, *J. Am. Chem. Soc.* **1990**, *112*, 4037-4038.

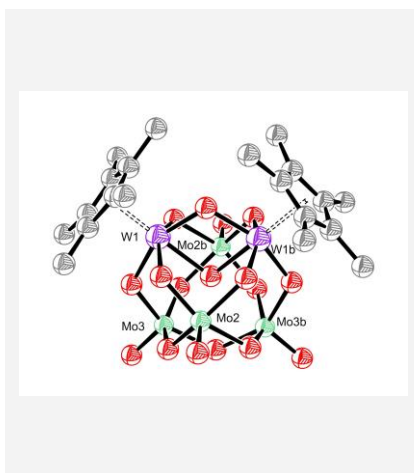
- [57] J.-E. Jee, A. Comas-Vives, C. Dinoui, G. Ujaque, R. Van Eldik, A. Lledós and R. Poli, *Inorg. Chem* **2007**, *46*, 4103-4113.
- [58] C. Rocchiccioli-Deltcheff, M. Fournier, R. Franck and R. Thouvenot, *J. Mol. Struct.* **1984**, *114*, 49-56.
- [59] C. Rocchiccioli-Deltcheff, R. Thouvenot and M. Fouassier, *Inorg. Chem.* **1982**, *21*, 30-35.
- [60] A. J. Bridgeman and G. Cavigliasso, *Chem. Phys.* **2002**, *279*, 143-159.
- [61] T. Roisnel and J. Rodríguez, *WINPLOTR*, <http://www.edifx.univ-rennes1.fr/winplotr/winplotr.htm>, **2009**.
- [62] M. J. Frisch, G. W. Trucks, H. B. Schlegel, G. E. Scuseria, M. A. Robb, J. R. Cheeseman, J. Montgomery, J. A., T. Vreven, K. N. Kudin, J. C. Burant, J. M. Millam, S. S. Iyengar, J. Tomasi, V. Barone, B. Mennucci, M. Cossi, G. Scalmani, N. Rega, G. A. Petersson, H. Nakatsuji, M. Hada, M. Ehara, K. Toyota, R. Fukuda, J. Hasegawa, M. Ishida, T. Nakajima, Y. Honda, O. Kitao, H. Nakai, M. Klene, X. Li, J. E. Knox, H. P. Hratchian, J. B. Cross, C. Adamo, J. Jaramillo, R. Gomperts, R. E. Stratmann, O. Yazyev, A. J. Austin, R. Cammi, C. Pomelli, J. W. Ochterski, P. Y. Ayala, K. Morokuma, G. A. Voth, P. Salvador, J. J. Dannenberg, V. G. Zakrzewski, S. Dapprich, A. D. Daniels, M. C. Strain, O. Farkas, D. K. Malick, A. D. Rabuck, K. Raghavachari, J. B. Foresman, J. V. Ortiz, Q. Cui, A. G. Baboul, S. Clifford, J. Cioslowski, B. B. Stefanov, G. Liu, A. Liashenko, P. Piskorz, I. Komaromi, R. L. Martin, D. J. Fox, T. Keith, M. A. Al-Laham, C. Y. Peng, A. Nanayakkara, M. Challacombe, P. M. W. Gill, B. Johnson, W. Chen, M. W. Wong, C. Gonzalez and J. A. Pople, *Gaussian 03, Revision D.01*, Gaussian, Inc., Wallingford CT, **2004**.
- [63] A. D. Becke, *J. Chem. Phys.* **1993**, *98*, 5648-5652.
- [64] C. T. Lee, W. T. Yang and R. G. Parr, *Phys. Rev. B* **1988**, *37*, 785-789.
- [65] B. Miehlich, A. Savin, H. Stoll and H. Preuss, *Chem. Phys. Lett.* **1989**, *157*, 200-206.
- [66] W. J. Stevens, M. Krauss, H. Basch and P. G. Jasien, *Can. J. Chem.* **1992**, *70*, 612-630.

Received: ((will be filled in by the editorial staff))
 Published online: ((will be filled in by the editorial staff))

Entry for the Table of Contents

Layout 1:

Room temperature assembly of the organometallic $\text{Cp}^*_2\text{M}_2\text{O}_5$ and the inorganic $\text{M}'\text{O}_4^{2-}$ under aqueous acidic conditions readily and selectively yields the organometallic oxides $\text{Cp}^*_2\text{M}_2\text{M}'_4\text{O}_{17}$ ($\text{M}, \text{M}' = \text{Mo}, \text{W}$) with a Lindqvist-type structure.



Mixed-Metal Organometallic Oxides

Gülnur Taban-Çalışkan, Dominique Agustin,* Funda Demirhan, Laure Vendier, and Rinaldo Poli*
Page No. – Page No.

Rational, facile synthesis and characterization of the neutral mixed-metal organometallic oxides $\text{Cp}^*_2\text{Mo}_x\text{W}_{6-x}\text{O}_{17}$ ($\text{Cp}^* = \text{C}_5\text{Me}_5$, $x = 0, 2, 4, 6$)

Keywords: Organometallic oxides / tungsten / molybdenum / polyoxometallates / DFT calculation / X-ray powder analysis